Journal of Interfaces, Thin films, and Low dimensional systems 3 (1) Summer and Autumn (2019) 219-226

Photocatalytic degradation of Congo red by ZnO nanoparticles with different morphology

Scientific research paper

Nasibeh Molahasani*

Department of Chemistry, East Tehran branch, Islamic Azad University, Tehran, Iran

ARTICLE INFO

Article history:
Received 22 May 2020
Revised 24 August 2020
Accepted 25 August 2020
Available online 10 September 2020

Keywords:
Nanoparticle
Zinc-Oxide
Absorption
Congo red
Photocatalyst

ABSTRACT

In this study, ZnO nanoparticles in three shapes, spherical, rod, and sheet are synthesized by a hydrothermal method using three different surfactants, namely three ethanol amine, cetyl three methyl ammonium bromide, and sodium dodecyl sulfate. In all cases, the chemical composition, powder identification, morphology. and particle size of the final product are characterized by Fourier transform infrared (FTIR), X-ray diffraction (XRD), field emission scanning electronic microscopy (FESEM), EDX elemental analysis, and UV-Vis spectroscopy. The photocatalytic activity of the nanoparticles are investigated for degradation of organic pollutants (Congo red dye). The removal tests of Congo red as a water organic pollutant indicates photocatalytic activity and absorption ability of synthesized zinc oxides. Finally, the comparison of the dye removal results show that the rod nanoparticle has more efficiency in the degradation of Congo red with 97% yield over 2 hours at pH=8.

1 Introduction

Researchers are developing low-cost and high-performance materials for the development of photocatalysts at the present time. Semiconductors such as ZnO nanostructures are appropriate candidates for catalyst applications because of their unique properties. One of the essential features of semiconductors is the ability to form electron-hole pairs by absorbing UV-Vis light. The energy of these charge carriers can be used in various ways, e.g. photocatalytic reactions. Organic and inorganic species can be reduced by emitted electrons. The formed holes can also oxidize the compound by taking electrons from the surface [1]. Heterogeneous catalysts have high efficiency for converting organic and inorganic pollutants into CO_2 and water [2, 3]. Removing dye is usually costly, inefficient, and only transfers contamination to other locations. Reduction of these pollutants with traditional methods is not complete because of the high solubility in water and their resistance to removal [4-6]. Therefore, to meet the future needs of the environment, the development of effective, non-toxic, environmentally friendly and sustainable photcatalyst is necessary. Zinc oxide with a wide band gap (3.37 eV) has the power to decompose many organic compounds [7, 8]. The oxidizing ability of ZnO is due to the production, mobility, and separation of photo-excited electrons and holes pairs, numerous point defects such as oxygen vacancies, hydroxyl ions production, and higher photo activity in both UV and sunlight irradiation [9-14]. Another advantage of zinc oxide is the ability to synthesize at low temperatures in various morphologies. Zinc oxide

*Corresponding author.
Email address: Nmolahasani@gmail.com
DOI: 10.22051/jitl.2020.31515.1039

nanoparticles is best suited for photocatalyst applications due to its more extensive surface area and ability to be suspended in the solution [15]. Also the size, crystallinity, and morphology of the particles can significantly influence the catalytic property [16-19]. Congo red (CR) was used as an azo dye to study the photocatalytic properties of zinc oxide. Due to its complex aromatic structure, Congo red is resistant to degradation, so it is important to find ways to remove it from waste waters [20]. The CR dye is one of the main pollutants in textile industries' water. This is because it has a stable structure and does not degrade easily. In the present study, the photocatalytic activity of ZnO nanoparticles is investigated by the photocatalytic discoloration of Congo red (CR) in aqueous solution. The particles were formed through the hydrothermal method in the presence of three different surfactant. Also the effect of particle morphology and pH on photocatalytic degradation of congo red is studied.

2 Experiment

Zn $(CH_3COO)_2$:$2H_2O$, Cetyl trimethyl ammonium bromide (CTAB), $ZnCl_2$:$6H_2O$, Potassium hydroxide (KOH), Sodium hydroxide (NaOH), NH_3, absolute ethanol, Sodium dodecyl sulfate (SDS), Tri ethanol amine (TEA), Congo red and HCl, purchased from the Merck Company and applied without further purification. Deionized and distilled water were used to prepare the solutions in this work. Sample preparation was carried out by the hydrothermal method.

2.1 Synthesis of ZnO nanoparticles by CTAB (R-NPs)

At first, 5.0×10^{-4} mol of $ZnCl_2$:$6H_2O$ and 1×10^{-3} mol of potassium hydroxide were dissolved separately in 2ml of distilled water by stirring at room temperature. A white calcic precipitation was formed immediately after mixing. Then, 25×10^{-5} mol of cetyl trimethyl ammonium bromide (CTAB) was added to the solution as a surfactant under stirring. The pH of the medium was about 8-9 at this step. After stirring for 5 minutes, the mixture was transferred to a 15 ml autoclave filled with distilled water and heated in an oven at 120 °C for 5 hours. When the time elapsed, the autoclave was cooled naturally. Then the solid-white reaction product was washed with distilled water and ethanol to remove impurities and non-reactive substances. It was dried in an oven for 5 hours at 50 °C and used for the stated analysis.

2.2 Synthesis of ZnO nanoparticles by TEA (SP-NPs)

2×10^{-3} mol of $ZnCl_2$:$6H_2O$ was first dissolved in 2.5ml of distilled water by stirring at room temperature. 2×10^{-3} mol (206×10^{-3} ml) of tri ethanol amine (TEA) was added as a surfactant to the reaction mixture. After 1.5 hours stirring, 4×10^{-3} mol KOH dissolved in 1.5 ml distilled water was added at room temperature. The reaction mixture was poured into a 15 ml autoclave with 11 ml of distilled water, and it was placed in an oven for about 5 hours at 120 °C. The autoclave was cooled naturally at room temperature. The white powder was treated with distilled water and ethanol to remove the probable impurities. The final product was dried in an oven for 5 hours at 50 °C and then used for characteristic analysis.

2.3 Synthesis of ZnO nanoparticles by SDS (S-NPs)

To synthesize ZnO nanoparticles by SDS, 5×10^{-4} mol of $ZnCl_2$ and 2×10^{-3} of KOH were dissolved in 20ml distilled water at room temperature. Then 25×10^{-5} mol of sodium dodecyl sulfate (SDS) was added to the stirring reaction mixture. The reaction mixture was then poured into the autoclave with some distilled water and placed in an oven at 120 °C for 5 hours. The autoclave was cooled naturally at room temperature, and the white powder was then treated with distilled water and ethanol to remove any impurities. After that, the final product was dried in an oven for 5 hours at 50 °C and then used for diagnostic analysis.

2.4 Photocatalytic activity measurements

The photocatalytic behavior of the zinc oxides was investigated under UV lamp (30W, UV-C, 253.7 nm, photon provides 4.89 eV). Photo degradation of 10 ppm Congo red solutions (as a model of water pollution) was determined by using a spectrophotometer at λ max= 496 nm. The lamp distance from the solution was 10 cm. For each experiment, 5×10^{-2} g of catalysts was dispersed into 100 ml of 10 ppm CR aqueous solution under stirring

to reach the adsorption equilibrium. The reaction vessel is simultaneously pumped by bubbles from the air pump (flow: 4.5 L in 1 min) to disperse the solution uniformly. After sampling at specific intervals (10 min for 2h), the catalyst was rapidly separated by centrifugation at 6000 rpm for 5 minutes. Then photocatalytic removal of the Congo red were followed by changing absorbance at $\lambda = 496$ nm.

The concentration of dye was determined by using a calibration curve. The percentage removal of CR is calculated as follows:

$$PD\% = (Ci - Ct)/Ci \times 100, \quad (1)$$

where, Ci is the initial concentration of the dye before exposure to the light source, and Ct is the concentration of the dye at any interval [21]. The photocatalyst recycling tests were performed in the same way and they were repeated four times. For this purpose, the suspension was sonicated for 5 min and then stirred in the dark place for 30–45 min to ensure an adsorption/desorption equilibrium was occurred.

3 Results and discussion

3.1 FESEM-EDAX Observations

The images of the as-synthesized samples are shown in Fig. 1a-1c. Effects of applying different surfactants on the morphologies of ZnO particles are revealed in the FESEM images. As seen, the morphology of the particles has the same distribution and dispersion. The shape of the particles is spherical, rod, and sheet like for TEA, CTAB, and SDS respectively.

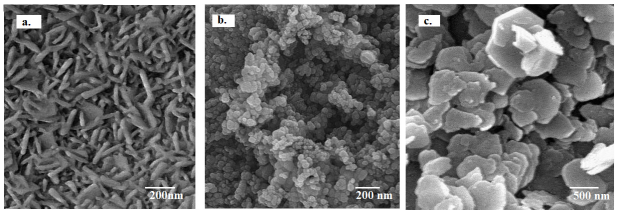

Figure 1. FESEM images of (a) R-NPs (b) SP-NPs (c) S-NPs.

From the FESEM results, the key roles of surfactants in controlling the particle morphology and crystal orientation can be seen. Surfactants can control nucleation, and also prevent the formation of agglomerates. The presence of these compounds affect not only nucleation and particle growth, but also coagulation and flocculation of the particles. The surfactant effect involves chelation of the metal cations of the precursor in an aqueous environment. CTAB is a cationic surfactant and produces a tetrahedral cation (CTA+) in an aqueous solution. Electrostatic interaction between CTA+ and zinc species leads to formation of nano-rods. It was found that CTAB affects the process of nucleation and growth of crystallites during synthesis, and also prevents the formation of agglomerates. As a non-ionic surfactant, TEA forms nano-ZnO in spherical-shape by weak Van der Waals interaction. On the other hand, SDS, as an anionic surfactant, affects the morphology of ZnO and turns it into a sheet. The presence of the surfactant was found to affect both the shape and size of the resulting ZnO particles which additionally suggests that the transformation may take place via a mechanism of recrystallization [22-25]. According to Fig. 1, the diameter of 1D nanostructure of R-NPs was found to be in between 23-38 nm. The FESEM images (Fig. 1b and c) reveal that SP-NPs have spherical shape with average size of 60 nm and S-NPs have sheet-like shape about 200nm. EDAX results indicated in Table 1, also confirm the presence of zinc and oxygen in stoichiometric ratios in the samples.

Table 1. Zn and O element content of the zinc oxide nanoparticles according to EDAX analysis.

Samples	Elements	Weight %	Atomic %
ZnO (rod) R-NPs	Zn	89.56	67.86
	O	10.44	32.14
ZnO (spherical) SP-NPs	Zn	89.68	67.56
	O	10.67	32.44
ZnO (sheet) SP-NPs	Zn	89.12	67.32
	O	10.88	32.68

3.2 XRD analysis

In Fig. 2a-2c, the XRD patterns of the as-obtained zinc oxide nanoparticles is shown. All of the peaks in the pattern illustrates the hexagonal structure of ZnO with high crystallity (hexagonal crystal system, P63 mc space group, JCPDS card No. 36-1451). The patterns show different peaks at about 2θ = 31.44, 34.41, 36.325, 47.87, 56.22, 62.11, 65.78, 67.13, 68.96, 72.23, 76.02, match the planes [100], [002],

[101], [102], [110], [103], [200], [112],[201], [004] and [202], which correspond the hexagonal structure of Zinc oxide [26]. The results revealed differences in peak intensities. The sharper peaks in Fig. 2b illustrate that ZnO particles constructed by TEA, enjoy higher crystallinity and purity. Samples synthesized with SDS show significant increase in the [002] plane and decrease in the [100] and [101] plane intensities compared to the other samples. This is due to different degrees of preferred growth orientation of the ZnO phase [27].

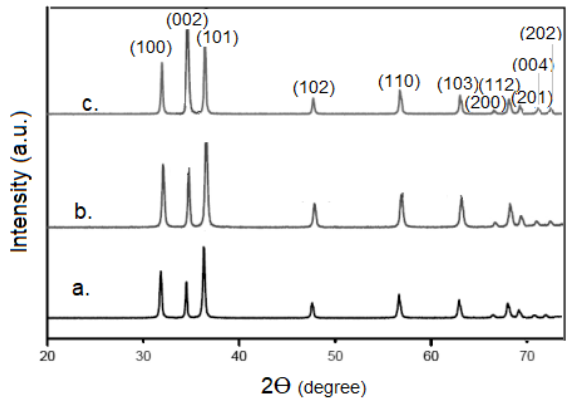

Figure 2. XRD patterns of Zinc oxide nanoparticles (a) R-NPs (b) SP-NPs (c) S-NPs.

All patterns also show no characteristic peaks of impurities such as surfactants or other Zinc oxides, so we can conclude that the formed ZnO has high purity. The crystallite sizes (D) of ZnO NPs calculate by Using Debye Scherer's formula are tabulated in Table 2 obtained by [28]:

$$D = K\lambda/\beta Cos\theta. \quad (2)$$

In Eq. (2), the parameter K= 0.94 is the space factor, λ= 1.5406 Å is the x- ray wavelength, θ is the Bragg diffraction angle and β is the full width at half-maximum in radians. Size calculation shows the crystallite sizes increase from 23 to 68 nm depending on the surfactant and shape.

Table. 2. Calculated crystallite size for the samples by Debye Scherer's formula.

Samples	ZnO (rod)	ZnO (spherical)	ZnO (sheet)
FWHMi	0.2362	0.2755	0.2018
2Θ	36.325	36.060	34.50
Crystaliite Size (nm)	35.3	30.3	41.2

3.3 UV-visible studies

The UV-Visible spectrum of zinc oxide nanoparticles in rod, spherical, and sheet-shape is represented in Figs. 3a-3c respectively. The absorbance edges observed for these spectrums are 360, 363, and 361 nm compared with the bulk ZnO which is 373 nm. In all the cases, blue shifts in wavelength were observed. The blue shift in the excitation absorbance clearly indicates the quantum confinement property of NPs [34]. Also, there was no peak in the spectrum except the characteristic peak, which suggests that ZnO NPs possess high purity.

3.4 Photocatalytic analysis

The photocatalytic properties of the prepared ZnO nanoparticles are studied using Congo red as a model dye under UV irradiation (30 W - λ = 254 nm). The lamp distance from the surface of solution is 10 cm. The batch experiments were carried out with 100 ml dye solutions (10 ppm) after adding 5×10^{-2} g catalyst under stirring. The UV-Vis spectrum of the CR, as seen in Fig. 3d the spectrum reveals two peaks at 346 nm and 496 nm. The absorption intensity at the λ max (496 nm) for 10 ppm CR solution is 0.285. We have used both UV and catalyst to analyze the photocatalytic behavior of nanostructures. Therefore, the progress of photo catalytic degradation was determined by measuring the absorbance of the solution samples by UV-Vis spectrophotometer at λmax = 496 nm. The percentage of degradation was calculated using the Eq. (1). Therefore, the changes in the absorption intensity at 496 nm were measured for different samples after catalyst removal.

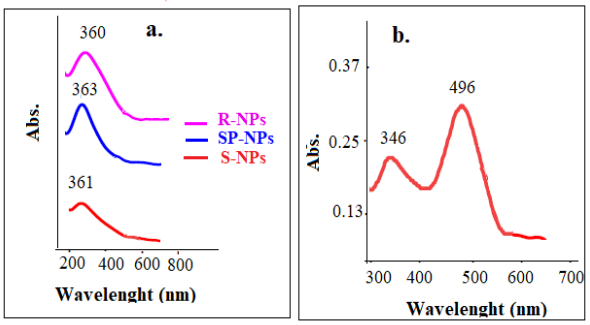

Figure 3. The absorption spectra of (a) Zinc oxide nanoparticles (b) Congo red.

As the irradiation time increases, the intensity of the characteristic peak decreases, indicating that the complete degradation of the dye by ZnO NPs occurred in about 2h, as shown in Fig. 4. We also examined the effects of each UV and catalyst factor separately on the CR degradation (Fig. 4). Finally, a number of tests were performed to explore the possibility of catalyst recovery.

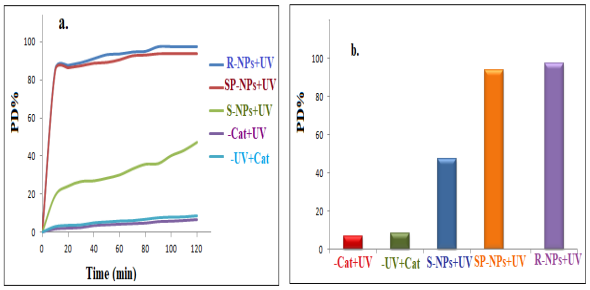

Figure 4. (a) Plot of photodegradation of CR versus reaction time (b) Comparison of PD % during 2h.

3.5 Effect of catalyst morphology and UV light on the photocatalytic activity

The photocatalytic applications of the ZnO catalysts is studied. A sample was placed on a beaker containing an aqueous solution of CR (pH=8). While being exposed to UV radiation the solution was mixed. Absorption was measured immediately before exposure to UV and at set time intervals, using a UV/Vis spectrophotometer. Figure 5 shows the efficiency of photo degradation (X) of the catalysts for the removal of CR as a function of time at λ = 496 nm. As shown in Fig. 4, the degradation of CR was slightly improved in absence of UV and catalyst, so the degradation rate was not more than 9% over two hours. The obtained results also showed that the PD% for R-NPs, SP-NPs, and S-NPs are 97.54, 93.68, and 47.37 respectively. The degradation rates of CR are indicative of considerable differences among ZnO samples synthesized by different morphologies. For example, the ZnO nano-rods exhibited the highest photocatalytic activity, as shown in Fig. 4, CR is almost completely degraded (998%) after exposure to the ultraviolet light for 2h but in the ZnO nanoparticles (S-NPs) underwent 47% degradation after 2h. These tests presented that the ZnO nano-rods (with UV) have

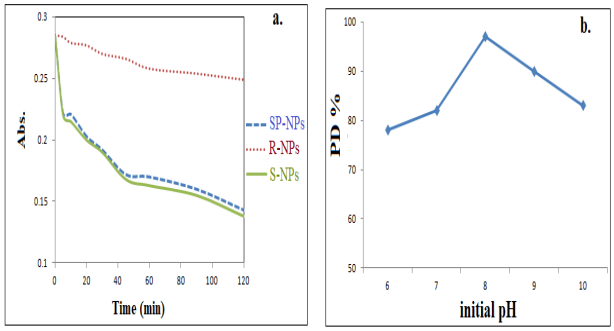

Figure 5. (a) investigation of UV removal on the photocatalytic activity of zinc oxide nanoparticles (b) Effect of initial pH on photodegradation rate of R-NPs.

slightly better photocatalytic properties compared with ZnO nano-sphere and nano-sheet. Some part of the dye removal by catalysts is due to surface adsorption, and a large part of it occurs by photocatalytic properties. As the results show, the broad surface of S-NPs is saturated with dye at the beginning of the experiment and its photocatalytic activity has decreased significantly. Fig. 5a shows the results of dye degradation by the catalysts in the absence of UV radiation. As can be seen from the results, the percentage of dye removal for the rod and spherical catalyst goes up to about 50% and for the sheet catalyst up to 13%. These results indicate the surface adsorption effect in the dye removal. However, as seen in this study, the photocatalytic properties of ZnO can be influenced by its morphology. The mechanism of photocatalytic reaction is [35-37]:

$ZnO + h\nu \rightarrow ZnO\ (e^{-}CB + h^{+}\nu B)$

$h^{+}\nu B + Dye \rightarrow$ oxidation of Dye molecule

$h^{+}\nu B + H_2O \rightarrow H^{+} + OH^{o}$

$h^{+}\nu B + OH^{-} \rightarrow OH^{o}$

$e^{-}CB + O_2 \rightarrow {}^{o}O_2^{-}$

${}^{o}O_2^{-} + Dye \rightarrow Dye—OO^{o}-$

${}^{o}O_2^{-} + HO_2^{o} + H^{+} \rightarrow H_2O_2 + O_2$

$OH^{o} + Dye \rightarrow$ oxidation of Dye molecule

3.6 Effect of pH on the photocatalytic activity of NPs

To investigate the effect of initial pH on photodegradation ability of R-NPs as a chosen catalyst, tests were performed at different pH (6-10) for preventing Congo red accumulation. Adjusting pH was done by adding appropriate amount of NaOH and HCl solution to the main test container. Other conditions such as CR concentration, temperature, doze of catalysts were kept constant over the experiments. Figure 5b showed that the pH values affect the photodecomposition percent of CR. As observed, the PD% raises from 78 to 97 as the pH increases from 6 to 8 before decreasing to 83 at pH=10. The best PD% was obtained at PH=8 that was selected as the pH tests. Actually, different PD% upon pH can be explained by surface modifications due to isoelectrical point (pH=9) that affects the surface charge of the semiconductor. Congo red as an onionic dye easily absorbs on the semiconductor surface in lower zero point charge (zpc) and repels at pH>zpc. So photoctalytic activity of Congo red reaches a maximum value in lower pH zpc [38, 39].

3.7 Effect of recovery cycle on the photocatalytic activity

Due to the importance of the recovery of the catalysts, especially in industrial processes, the zinc oxide used in each experiment was recrystallized and placed in an autoclave at 120 °C for 5h to remove the adsorbed dyes. Then their photocatalytic activity was reassessed for two hours. The results showed (Fig. 6) that the catalytic activity of the Zinc oxides does not change significantly after the four recovery times.

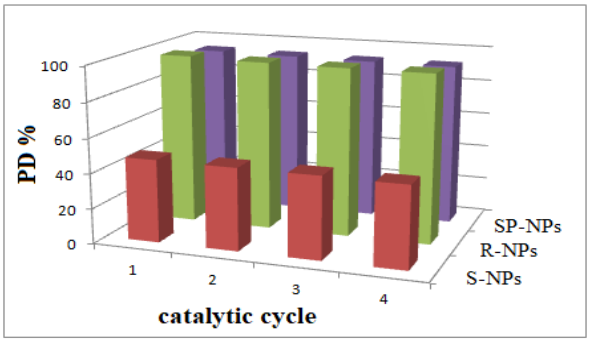

Figure 6. Recyclability of the catalysts.

3 Conclusions

In this study, the synthesis of zinc oxide nanoparticles in spherical, rod, and sheet-form for photocatalytic purposes was performed. Investigations with FESEM-EDX, XRD, FTIR, and UV-Vis indicate nanometer size and suitable shape for the use. The percent degradation of Congo Red exposed to UV radiation was achieved by nano-oxide on a rod 97.54%, spherical nano oxide 93.68%, and sheet nano-oxide 48%, which the highest value is for rod zinc oxide at pH=8. The results of dye removal showed the maximum degradation in the presence of both catalyst and UV light. So, the amount of adsorption decreases and the degradation increases under both agents. According to the results, it can be obtained that PD% depend upon the pH and the catalysts can be used at least four times in a photocatlytic reaction.

Acknowledgments

The author much acknowledges to the vice presidency of Islamic Azad University, East Tehran branch for their encouragement and financial supports from this internal project.

References

[1] N. S. Lewis, “Research opportunities to advance solar energy utilization.” Science, **351** (2016) 1920.

[2] A. Eslami, S. Nasseri, B. Yadollahi, A. Mesdaghinia, F. Vaezi, et al. “Enhanced ozonation of dichloroacetic acid in aqueous solution using nanometer ZnO powders” Journal Chemical and Technology Biotechnology, **83** (2008) 1447.

[3] N. Laouedj, A. Bekka, B. Elaziouti, et al. “ZnO-Assisted Photocatalytic Degradation of Congo Red and Benzopurpurine 4B in Aqueous Solution” Journal of Chemical Engineering & Process Technology, **2** (2011) 2.

[4] C.I. Pearce, J.R. Lloyd, J.T. Guthrie, “The removal of colour from textile wastewater using whole bacterial cells: a review.” Dyes and Pigments, **58** (2003) 179.

[5] T. Robinson, G. Mcmullan, R. Marchant, P. Nigam, “Remediation of dyes in textile effluent: a critical review on current treatment technologies with a

proposed alternative." Bioresourse Technology, **77** (2001) 247.

[6] Y.H. Leung, A.M. Ching. "Strategies for improving the efficiency of semiconductor metal oxide photocatalysis." Materials Horizons, **1** (2014) 400.

[7] M. Miyauchi, A. Nakajima, T. Watanabe, K. Hashimoto, "Photocatalysis and Photoinduced Hydrophilicity of Various Metal Oxide Thin Films." Chemistry of Materials, **14** (2002) 2812.

[8] A. Ravanbakhsh, F. Rashchi, M. Heydarzadeh Sohi, R. Khayyam Nekouei, M. Mortazavi Samarin "Synthesis and characterization of porous zinc oxide nano-flakes film in alkaline media." Journal of Ultrafine Grained and Nanostructured Materials, **51** (2018) 32.

[9] S. Merouani, O. Hamdaoui, F. Saoudi, M.S. Chiha, "Sonochemical degradation of Rhodamine B in aqueous phase: Effects of additives." Chemical Engineering Journal, **158** (2010) 550.

[10] V. Kandavelu, H. Kastien, K.R. Thampi, "Photocatalytic degradation of isothiazolin-3-ones in water and emulsion paints containing nanocrystalline TiO_2 and ZnO catalysts" Applied Catalysis B: Environmental, **48** (2004) 101.

[11] A. Abdel Aal, S.A. Mahmoud, A.K. Aboul-Gheit, "Sol–Gel and Thermally Evaporated Nanostructured Thin ZnO Films for Photocatalytic Degradation of Trichlorophenol." Nanoscale Research Letters. **4** (2009) 627.

[12] B. Neppolian, S. Sakthivel, B. Arabindoo, M. Palanicham, V. Murugesan, "Degradation of textile dye by solar light using TiO_2 and ZnO photocatalysts." Journal of Environmental Science and Health, Part A. **34** (1999) 1829.

[13] I. Udom, M.K. Ram, E.K. Stefanakos, A.F. Hepp, D.Y. Goswami, "one dimential ZnO nanostructures." Material Science in Semiconductor Processing, **16** (2013) 2070.

[14] N. Smirnova, Y. Gnatyuk, A. Eremenko, G. Kolbasov, V. Vorobetz, I. Kolbasova, O. Linyucheva, "Photoelectrochemical and photocatalytic properties of mesoporous TiO_2 films modified with silver and gold nanoparticles." International Journal of Photoenergy, **1** (2006) 1205.

[15] M. Bagheri, A.R. Mahjoub, B. Mehri, "Enhanced photocatalytic degradation of congo red by solvothermally synthesized $CuInSe_2$–ZnO nanocomposites." RSC Advances, **4** (2014) 21757.

[16] Y. Li, W. Xie, X. Hu, G. Shen, X. Zhou, Y. Xiang, et al. "Comparison of Dye Photodegradation and its Coupling with Light-to-Electricity Conversion over TiO_2 and ZnO." Langmuir, **26** (2010) 591.

[17] P.E. de Jongh, E.A. Meulenkamp, D. Vanmaekelbergh, J.J. Kelly, "Charge Carrier Dynamics in Illuminated, Particulate ZnO Electrodes." The Journal of Physical Chemistry B, **104** (2000) 7686.

[18] Y. Cui, C.M. Lieber, "Functional nanoscale electronic devices assembled using nanowire blocks." Science. **29** (2001) 851.

[19] P. Sukanta, S. Mondal, J. Maity, R. Mukherjee, "Synthesis and Characterization of ZnO Nanoparticles using Moringa Oleifera Leaf Extract: Investigation of Photocatalytic and Antibacterial Activity." International Journal of Nanoscience and Nanotechnology, **14** (2018) 111.

[20] R. Ramakrishnan, S. Kalaivani, J. Amala Infant Joice, T. Sivakumar, "Photocatalytic activity of multielement doped TiO_2 in the degradation of congo red." Applied Surface Science, **258** (2012) 2515.

[21] S. Aghabeygi, Z. Sharifi, N. Molahasani, "Enhanced photocatalytic property of nano-ZrO_2-SnO_2 NPs for photodegradation of an azo dye." Digest Journal of Nanomaterials and Biostructures, **12** (2017) 1.

[22] H. Usui. "The effect of surfactants on the morphology and optical properties of precipitated wurtzite ZnO." Materials Letters, **63** (2009) 1489.

[23] S. Lv, C. Wang, T. Zhou, S. Jing, Y. Wu, C. Zhao, "In situ synthesis of ZnO nanostructures on a zinc substrate assisted with mixed cationic/anionic surfactants." Journal of Alloys Compounds, **477** (2009) 364.

[24] Y. Ni, G. Wu, X. Zhang, X. Cao, G. Hu, A. Tao, Z. Yang, X. Wei, "Hydrothermal preparation, characterization and property research of flowerlike ZnO nanocrystals built up by nanoflakes." Materials Research Bulliten, **43** (2008) 2919.

[25] U.N. Maiti, S. Nandy, S. Karan, B. Mallik, K.K. Chattopadhyay, "Enhanced optical and field emission properties of CTAB-assisted hydrothermal grown ZnO nanorods." Applied Surface Science, **254** (2008) 7266.

[26] S. Aghdasi, M. Shokri, "Photocatalytic degradation of ciprofloxacin in the presence of synthesized ZnO nanocatalyst: The effect of operational parameters." Iranian Journal of Catalysis, **6** (2016) 481.

[27] E.M.P. Steinmiller, K.S. Choi, "Anodic Construction of Lamellar Structured ZnO Films Using Basic Media via Interfacial Surfactant Templating." Langmuir, **23** (2007) 12710.

[28] K. Zare, N. Molahasani, N. Farhadyar, M.S. Sadjadi, "Enhanced Blue Green Emission of ZnO Nanorods Grown byHydrothermal Method." Journal of Nano Research, **21** (2013) 43.

[29] A.J.M. de Man, B.W.H. van Beest, M. Leslie, R.A. van Santen, "Lattice dynamics of zeolitic silica polymorphs." Journal of Physical Chemistry, **94** (1999) 2524.

[30] M.S. Sadjadi, A. Azimi, K. Zare, "Synthesis and Characterization of ZnO nanorods by Acrylamide Gel Method (AGM)." The Research Journal of Chemistry and Environment, **15** (2011) 856.

[31] M.S. Sadjadi, N. Farhadyar, K. Zare "Synthesis of ZnS/SiO2 Core-Shell by Sol-Gel Process and Covering then with Gold Nanoparticle and Study of its Photoluminescence Properties." Defect and Diffusion Forum, **1** (2012) 238.

[32] P. Rainho, J. Rocha, L.D. Carlos, R.M. Almeida, "Nuclear-Magnetic-Resonance and Vibrational Spectroscopy Studies of SiO_2-TiO_2 Powders Prepared by the Sol-Gel Process." Journal of Materials Research, **16** (2001) 2369.

[33] S.H. Ehrman, S.K. Friedlander, and M.R. Zachariah, "Phase segregation in binary SiO_2/TiO_2 and SiO_2/Fe_2O_3 nanoparticle aerosols formed in a premixed flame." Journal of Materials Research, **14** (1999) 4551.

[34] M.K. Debanath, S. Karmakar, "Biogenic ZnO nanoparticles: a study of blueshift of optical band gap and photocatalytic degradation of reactive yellow 186 dye under direct sunlight." Materials Letters, **111** (2013) 116.

[35] J. Talat- Mehrabada, M. Partovib, F. Arjomandi Rada, R. Khalilnezhad, "Nitrogen doped TiO_2 for efficient visible light photocatalytic dye degradation." Iranian Journal of Catalysis, **9** (2019) 233.

[36] H.R. Pouretedal, M. Fallahgar, F. Sotoudeh Pourhasan,M. Nasiri, "Taguchi optimization of photodegradation of yellow water of trinitrotoluene production catalyzed by nanoparticles TiO_2/N under visible light." Iranian Journal of Catalysis, **7** (2017) 317.

[37] F. Soori, A. Nezamzadeh-Ejhieh, "Photodegradation and antibacterial properties of zeolite cerium oxide nanocomposite." Journal of Molecular Liquids, **255** (2018) 250.

[38] B. Swarnalatha, Y. Anjaneyulu "Studies on the heterogeneous photocatalytic oxidation of 2,6-dinitrophenol in aqueous TiO_2 suspension." Journal of Molecular Catalysis A: Chemistry, **223** (2004) 161.

[39] C.E. Bonancea, G.M. Do Nascimento, M.L. De Souza, M.L.A. Temperini, P. Corio " Photodegradation of Congo red in aqueous solution on ZnO as an alternative catalyst to TiO_2." Applied Catalysis B: Environmental, **69** (2006) 3.